THE REMOVAL OF PERFLUOROOCTANOIC ACID AND PERFLUOROOCTANESULFONATE USING METAL-ORGANIC FRAMEWORKS

A Thesis

Presented to

The Faculty of the Department of Chemistry and Biochemistry

California State University, Los Angeles

In Partial Fulfillment

of the Requirements for the Degree

Master of Science

in

Chemistry

By

Hannah Tjitradjaja

August 2023

© 2023

Hannah Tjitradjaja

ALL RIGHTS RESERVED

The thesis of Hannah Tjitradjaja is approved.

Yangyang Liu, Ph.D., Committee Chair

Matthias Selke, Ph.D.

Petr Vozka, Ph.D.

Yixian Wang, Ph.D.

Krishna Foster, Ph.D., Department Chair

California State University, Los Angeles

August 2023

ABSTRACT

The Removal of Perfluorooctanoic Acid and Perfluorooctanesulfonate using Metal-Organic Frameworks

By

Hannah Tjitradjaja

Per- and polyfluoroalkyl substances (PFAS) are toxic contaminants found in multiple everyday products that bioaccumulate in humans, animals, and the environment causing many different health issues. PFAS are highly resilient, and current degradation methods are inadequate for removal, require high energy, and are not cost-efficient. Specifically, water treatments use activated carbons and ion-exchange resin as an adsorption method but are not designed to degrade PFAS. Waste after treatments also can re-contaminate landfills because the PFAS are just being relocated. The most frequently detected contaminants of PFAS are perfluorooctanoic acid (PFOA) and perfluorooctanesulfonate (PFOS). This project aims to degrade and remove PFOA and PFOS through photocatalytic reactions using metal-organic frameworks (MOFs) with nanoporous structures. These experiments will provide insights into water treatment methodology to degrade or remove PFAS more efficiently in hopes of reducing bioaccumulation and health effects in the future.

ACKNOWLEDGMENTS

I would like to thank Dr. Liu for the guidance and support she has given me while being a part of her lab. I also thank my labmates for giving me a supportive environment to grow and learn. Likewise, I want to thank Dr. Jiang for teaching me about instrumentation functionality and maintenance. Furthermore, I would like to thank my committee members: Dr. Selke, Dr. Wang, and Dr. Vozka, for their valuable feedback. I would also like to thank the National Science Foundation CREST program (Award Numbers HRD-1547723 and HRD-2112554) for financial support throughout my Master's program.

TABLE OF CONTENTS

Abstract …… iv

Acknowledgments ...…….. v

List of Figures ……. vii

Chapter

1. Introduction……...……. 1

    Significance …….……. 3

    Research Objective …….. 4

2. Methods ……...……..... 5

    Instrumentation ……. 5

    Synthesis of In-TCPP ……. 6

    Synthesis of PCN-222 ……... 6

    Preparation of Stock Solutions …… 7

    Adsorption of PFAS ……. 8

    Catalytic Photodegradation of PFAS …… 8

3. Results & Discussion …….. 10

    Characterization ……. 10

    LCMS Analysis ……...… 11

4. Future Work …… 18

5. Conclusion …….. 19

References ……...… 20

LIST OF FIGURES

Figures

1. General pathway of PFAS exposure ..…. 1
2. Crystal structure of NU-1000 with possible PFBS adsorption interaction …….. 3
3. Proposed schematic of PFOA adsorption on In_2O_3 and TiO_2 ……..… 4
4. Powder X-ray Diffraction Spectra …….. 10
5. N_2 isotherms of In-TCPP and PCN-222 ….....……. 11
6. PXRD of In-TCPP after storage……... 12
7. PFOA adsorption LCMS data ……..……... 13
8. PFOS adsorption LCMS data ……..……... 14
9. UV-Vis spectra and LCMS data of PFOA photocatalysis ……...…... 15
10. PFOS photocatalysis LCMS data ……... 16
11. PXRD after adsorptions …….. 17

CHAPTER 1

Introduction

In recent years, toxic man-made compounds, per- and poly-fluoroalkyl substances (PFAS), are gathering considerable attention in search of a degradation pathway. PFAS have been used for decades and are found in everyday and environmental items such as cookware, drinking water, pesticides, dust, and air (Figure 1).[1,2] These compounds are also being released to wastewater treatment plants with little management for human and environmental exposures. Exposures to these chemicals can accumulate in both the human body and the environment without breaking down for an undesirable amount of time.[1,3] This is because PFAS are very stable compounds with a strong carbon-fluorine bond.[4] The resulting accumulation can cause many different health effects, including cancer and dysfunction of the immune and hormonal systems.[2,4]

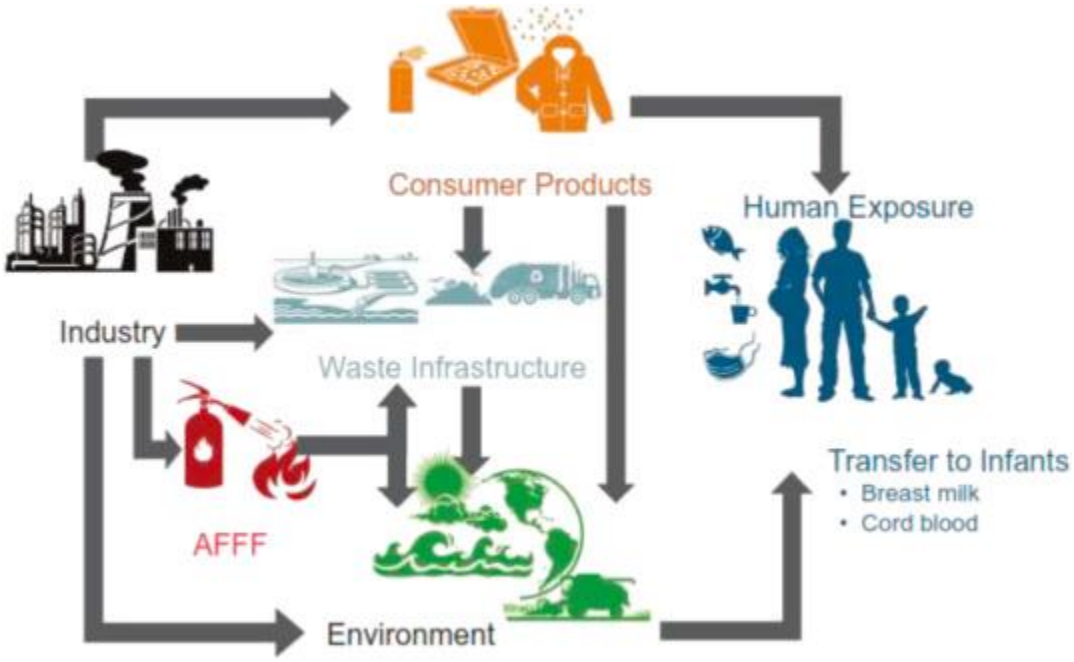


Figure 1. Pathways of different PFAS exposures lead to our daily encounters. Adapted from ref. 1 Copyright 2011 Royal Society of Chemistry.

Current water purification treatments are not designed to remove these toxic chemicals.[2,5] PFAS degradation methods include adsorption, filtration, reverse osmosis, photolysis, electrochemical oxidation, and sonochemical destruction. These methods have shown inadequate removal rates, require high energy, and are very expensive to perform.[6,7] Water treatment utilizes the adsorption method with activated carbons and ion exchange resins, which is inefficient and/or does not remove PFAS, as stated before.[7] This method is also not cost-efficient because the activated carbons and ion-exchanged resins are needed to be changed frequently.[7] Also, after water treatments, the waste is usually added back into the landfills, causing re-contamination.[1,2] Some initial findings in the properties of PFAS suggest that the carbon chain length can create a pathway for safer alternatives.[1] Shorter-chain PFAS would be preferred over long-chain PFAS because of its shorter half-lives.[6] Moreover, PFAS have functional groups that can be either hydrophobic or hydrophilic, which contributes to the resilience of these compounds from breaking down.[1] Removal of PFAS from water is believed to be achievable by using porous materials such as metal-organic frameworks (MOFs). Considering that MOFs have a highly porous feature[5] and some MOFs are very stable,[2] they are expected to be more effective in capturing and degrading toxic chemicals from water.[6]

MOFs are constructed from organic and inorganic elements that can be used for many different applications. MOFs have metal nodes and organic ligands that can create hydrophobic pockets (Figure 2A).[6] By coordinating the metals with other organic ligands, the surface of pores permits the framework to undergo various interactions for both the hydrophobic and hydrophilic functional groups of PFAS (Figures 2B and 2C).[6] The higher surface area of MOFs has been found to increase hydrophobic interactions that can influence the breakdown of PFAS with long carbon chains.[6] Various pore sizes also allow access to the

binding sites of MOFs (Figures 2D and 2E).[8] This can be an issue for larger molecules when pore sizes are too small.[8] With MOFs, the adsorption method was promising with short equilibrium times.[6] This finding also indicated that MOFs needed an ideal combination of porosity and node composition to demonstrate that the adsorption capabilities are not affecting the ability of the structure to regenerate. However, the structure-property interaction mechanisms of MOFs and PFAS are still being researched. This project studies the PFAS removal by photoactive MOFs with porphyrin linkers, which was not studied before.

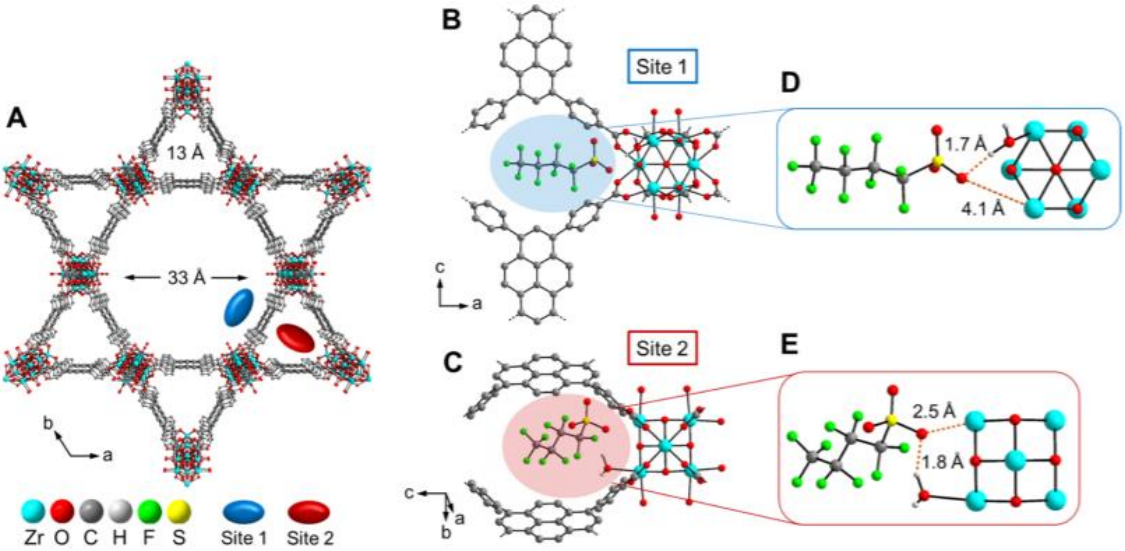


Figure 2. A. The crystal structure of NU-1000 with possible perfluorobutane sulfonate (PFBS) adsorption interaction. B. PFBS-pyrene linker-Zr_6 node interaction domain of site 1. C. Interaction site 2 of PFBS-pyrene linker-Zr_6 node. D. Zoomed-in adsorption site 1 interaction. E. Zoomed-in adsorption site 2 interaction. Adapted from ref. 6. Copyright 2021 American Chemical Society.

Photodegradation is theoretically better than adsorption because it will allow the removal of PFAS entirely instead of a transfer, which results in less waste that needs further treatment.[3,5] Metal oxides were previously studied for the photodegradation of PFAS.[1,4] Using metal oxide semiconductors allows for electron-hole separation when exciting the electron from the valence band to the conduction band.[1,4] The positively charged holes can move from one atom to another as electrons leave their position, leading to the reaction with PFAS

(Figure 3).[3] Similarly, MOFs' photoactive function allows reactive oxygen species (ROS), such as superoxide anion and hydroxyl radicals, to produce under light.[3,9] These ROS and other radicals are hypothesized to lead to the degradation of captured PFAS. However, very few studies have investigated the degradation of PFAS using MOFs. This project will study the photocatalytic degradation of PFOA and PFOS by photoactive MOFs bearing porphyrin linkers under blue LED.

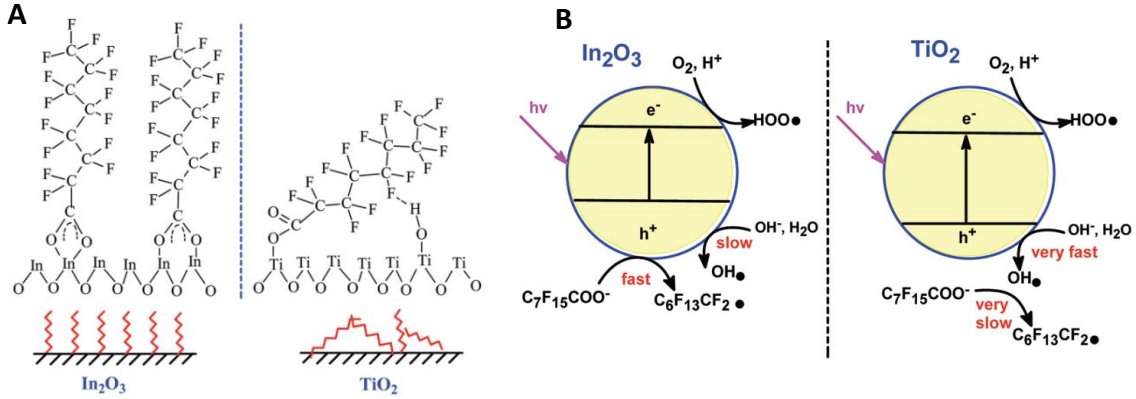


Figure 3. A. Proposed schematic of PFOA adsorption on In_2O_3 and TiO_2. B. Proposed mechanism of photocatalytic decomposition of PFOA. Adapted from ref. 3. Copyright 2012 American Chemical Society.

CHAPTER 2

Methods

Materials

Formic Acid (99%) was purchased from Acros Organics. *N, N*-dimethylformamide (DMF, 99.9%), benzoic acid (BA, 99.5%), indium (III) nitrate trihydrate ($In(NO_3)_3 \cdot H_2O$, 99.9%), and trifluoroacetic acid (TFA, 99.5%) were purchased from Fisher Scientific. Meso-tetra(4-carboxyphenyl)porphyrin (TCPP, 97%) was purchased from Frontier Scientific. Zirconium chloride ($ZrCl_4$ >99.5%) and perfluorooctanoic acid (PFOA, 95%) was obtained from Alfa Aesar. Perfluorooctanesulfonic acid in H_2O solution (PFOS, 41.6%) was purchased from Sigma-Aldrich.

Instrumentation

Powder X-ray diffraction (PXRD) data were collected on a D2 Phaser equipped with a Cu-sealed tube ($\lambda = 1.54178$) at 30 kV and 10 mA. The scan range was from 2-20° and a step size of $2\theta = 0.01°$, 1 second per step. The MOFs' nitrogen isotherms (77 K) and Brunauer-Emmett-Teller (BET) surface areas were measured on a Micromeritics ASAP 2020 Plus. Degas conditions consist of an evacuation phase and a heating phase. During the evacuation phase, the temperature ramp rate was 10.0° C per minute until reaching 100° C. The evacuation rate was at 5.0 mmHg per second until reaching a vacuum level of 10 μmHg for 60 minutes. During the heating phase, the ramp rate was at 10° C per minute at a hold temperature of 120° C for 720 minutes. Both evacuation and heating phases were at a hold pressure of 100 mmHg. Analysis for the isotherms was taken from 0.0005 relative pressure to 0.995 relative pressure, consisting of 35 adsorption points and 27 desorption points.

LED irradiation setup was fabricated on-site by mounting LEDs purchased from RapidLED into an aluminum base. The LEDs were connected in series to a Mean Well LPC-

35-700 constant current driver purchased from RapidLED. The aluminum base holds four CREE XT-E Royal Blue LEDs facing each other approximately 3 cm apart. The power density of each blue LED is 200 mW/cm^2.

PFAS concentration was measured using Thermoscientific Orbitrap Liquid Chromatography Mass Spectrometry (LCMS). The scan parameters were under negative polarity over the range of 100 to 600 m/z with two microscan steps. The electrospray ionization (ESI) source parameters were run with a sheath gas flow rate of 10 mL per minute, an auxiliary gas flow rate of 2 mL per minute with a spray voltage of 2.80 kV, and a capillary temperature of 275° C. The injection speed for the syringe was 10 µL per minute. Washing of the LCMS columns before, between, and after samples were conducted under similar ESI parameters except for a sheath gas flow rate of 35 mL per minute and a syringe injection rate of 100 µL per minute. Between samples, the syringe was washed five times.

Synthesis of In-TCPP

Preparation of In-TCPP followed procedures reported by Rhauderwiek et al.[10] In a pressure vessel, 60.0 mg of $In(NO_3)_3$ was dissolved in 378 µL DI water. 75.0 mg of TCPP and 3.6 mL of DMF were added and sonicated for 20 minutes. The solution was heated at 120° C for 48 hours, then cooled to room temperature. The MOF was washed with DMF three times, the first two washes for an hour and the last overnight. Acetone was used as a solvent exchange wash three times, the first two were washed for an hour, and the last was overnight. The material was dried in a vacuum oven overnight at room temperature.

Synthesis of PCN-222

The preparation of PCN-222 followed the procedures reported by Hao et al.[11] 14 mg of $ZrCl_4$, 20 mg of TCPP, 5.64 mL of formic acid, and 20 mL of DMF was added into a pressure

vessel and sonicated for 20 minutes. The solution was heated at 120° C for 18 hours, then cooled to room temperature. The MOF was washed with DMF three times, the first two washes for an hour, and the last overnight. Acetone was used as a solvent exchange wash three times, the first two were washed for an hour, and the last was overnight. The material was dried in a vacuum oven overnight at room temperature.

Preparation of Stock Solutions

PFOA. Procedures were adapted from Li et al.[6] 100 ppm stock solution of PFOA was made by dissolving 2.5 mg of PFOA in 25 mL of 50:50 ratio of MeOH and DI water. The 5 ppm stock solution was made from the 100 ppm stock solution, diluted to 10 mL. From the 5 ppm stock solution, 2 mL solutions (used for the calibration curve) ranging from 0.05 ppm to 5 ppm were made. Each solution included 2 µL of TFA solution in the total 2 mL solution. A 2000 ppm stock solution was made by dissolving 4 mg of PFOA in 2 mL of DI water.

PFOS. Procedures were similar to the PFOA procedure. The 100 ppm stock solution was made by diluting 6.01 µL of the PFOS solution to 25 mL with the 50:50 ratio of MeOH and DI water. From the 100 ppm stock solution, 5 ppm stock solution was diluted to 10 mL. The 5 ppm stock solution was used to prepare other solutions used for the calication curve, ranging from 0.05 ppm to 5 ppm. Each solution included 2 µL of TFA solution in the total 2 mL solution. A 2000 ppm stock solution was made by diluting 9.62 µL of the PFOS solution to 2 mL.

TFA. TFA stock solution was used as an internal standard for LCMS analysis. The TFA solution for PFOA was diluted to 500 ppm using the 50:50 ratio MeOH and DI water. When 2 µL of TFA solution was used, the total concentration would be 0.5 ppm in the 2 mL samples. For PFOS, the TFA solution needed to be more concentrated and therefore was diluted to 20,000 ppm, resulting in each sample being 20 ppm.

Adsorption of PFAS

PFOA. 100 ppm of PFOA was prepared by dissolving 2.5 mg of PFOA in 25 mL of DI water. This solution was added into a centrifuge tube and wrapped in foil. 5 mg of MOF was added to the centrifuge tube, shaken, and an aliquot was taken using a micropipette. The centrifuge tube was placed on a shaker plate. Aliquots were taken again at 5 and 30 minutes. Aliquots taken were 100 µL and filtered into a volumetric flask. 2 µL of 500 ppm TFA was added to the volumetric flask, which was then diluted to 2 mL using a 50:50 mixture of MeOH and DI water. These samples were then analyzed using the orbitrap LCMS.

PFOS. The 100 ppm of PFOS used was prepared similar from the 25 mL solutions from the stock, but diluted with DI water. This was added into a centrifuge tube and wrapped in foil. 5 mg of MOF was added to the centrifuge tube, shaken, and an aliquot was taken using a micropipette. The centrifuge tube was placed on a shaker plate. Aliquots were taken again at 5 and 30 minutes. All aliquots taken were 100 µL and filtered into a volumetric flask. 2 µL of 20,000 ppm TFA was added to the volumetric flask, which was then diluted to 2 mL using a 50:50 mixture of MeOH and DI water. These samples were then analyzed using the orbitrap LCMS.

Catalytic Photodegradation

PFOA. Procedures were adapted from procedures reported by Hao et al.[11] 5 mL of DI water and 1 mg of MOF were added into a microwave vial with an aluminum crimp cap and sonicated for 20 minutes. The solution was saturated with O_2 for 20 minutes. Using a microsyringe, 250 µL of 2000 ppm of PFOA was inserted into the solution, shaken, and an aliquot was taken. The solution underwent a blue LED irradiation with aliquots taken at 5 and 30 minutes. All aliquots taken with the microsyringe were 100 µL and filtered into a volumetric flask. 2 µL of 500 ppm TFA was added to the volumetric flask, which was then

diluted to 2 mL using a 50:50 mixture of MeOH and DI water. These samples were then analyzed through the orbitrap LCMS.

PFOS. Like the PFOA procedures, 5 mL of DI water and 1 mg of MOF were added into a microwave vial with an aluminum crimp cap and sonicated for 20 minutes. The solution was saturated with O_2 for 20 minutes. Using a microsyringe, 250 µL of 2000 ppm PFOS was inserted into the solution, shaken, and an aliquot was taken. The solution underwent a blue LED irradiation with aliquots taken at 5 and 30 minutes. All aliquots taken with the microsyringe were 100 µL and filtered into a volumetric flask. 2 µL of 20,000 TFA was added to the volumetric flask, which was then diluted to 2 mL using a 50:50 mixture of MeOH and DI water. These samples were then analyzed using the orbitrap LCMS.

CHAPTER 3

Results & Discussion

Materials Characterizations

Both MOFs were first characterized using PXRD for framework structures and compared to the simulated pattern from the Crystallographic Information File provided by the CCDC. The experimental PXRD patterns were shown to match the simulated patterns, indicating that the synthesis of the MOFs was successful (Figure 4).

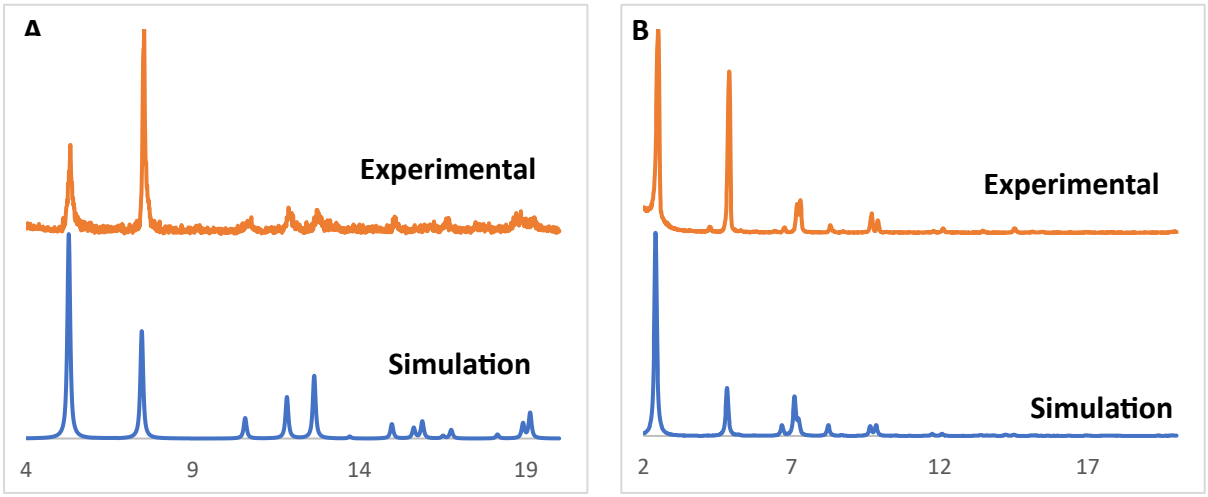


Figure 4. Simulated and Experimental PXRD spectra patterns of A. In-TCPP and B. PCN-222.

In addition, the surface areas of the synthesized MOFs were obtained from N_2 isotherm analysis at 77 K. The N_2 isotherms were compared to previous literature values and the Brunauer-Emmette-Teller (BET) surface area was calculated using the density functional theory (DFT). The experimental isotherm for both MOFs had good agreement with literature values (Figure 5). The experimental BET surface area for In-TCPP was 1114.9 m^2/g, matching literature values that were between 1100 and 1400 m^2/g.[10] For PCN-222, the experimental BET surface area was 2210.2 m^2/g, similar to literature value of 2223 m^2/g.[8]

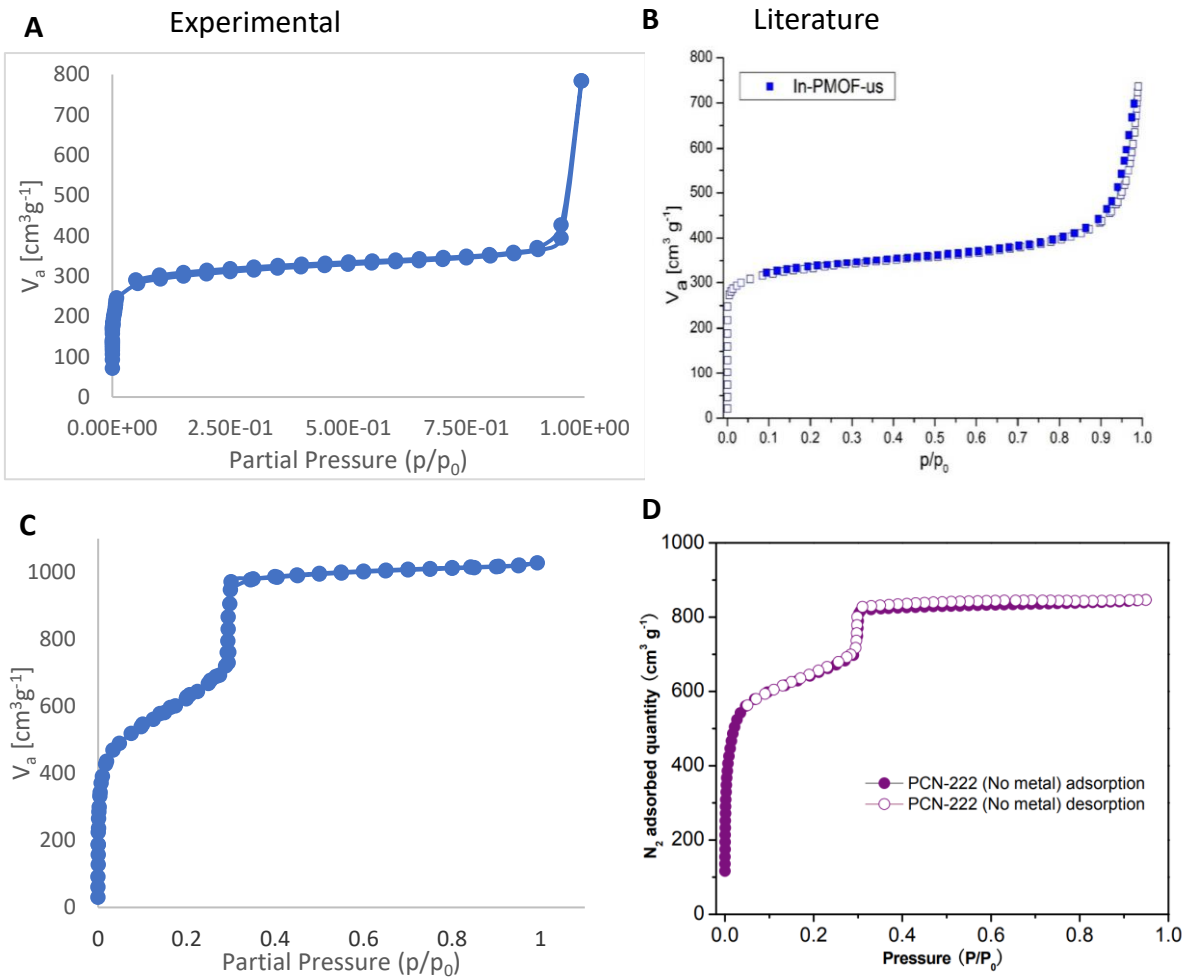


Figure 5. A. Experimental N_2 isotherm of In-TCPP. B. Literature N_2 isotherm for In-TCPP. C. Experimental N_2 isotherm for PCN-222. D. Literature N_2 isotherm for PCN-222. Copyright 2016 American Chemical Society. Copyright 2012 Wiley-VCH Verlag GmbH & Co. KGaA, Weinheim.

PFAS Adsorption Analysis

This research investigates MOFs that were not previously studied for PFAS adsorption. Inspired by PFOA decomposition using indium oxide, previously reported by Li et al., we first investigated an indium MOF for this project.[3] Keum et al. and many others have reported that photoactive MOFs could generate ROS, which may be capable of degrading PFAS.[9] We first conducted PFOA adsorption experiments using the In-TCPP MOF synthesized. After multiple attempts, the results obtained from LCMS analysis were inconclusive. We suspected the In-TCPP MOF may have undergone structural change during

the experiments. Therefore, another PXRD was done to look into the structure of the In-TCPP after the adsorption experiments. As shown in Figure 6, the PXRD pattern of the In-TCPP MOF after the adsorption experiments is different from the simulated pattern (missing a few peaks), indicating that the MOF was not stable in water and had decomposed during the adsorption experiments. Therefore, we determined that In-TCPP is not suitable for PFAS adsorption/degradation due to its poor stability.

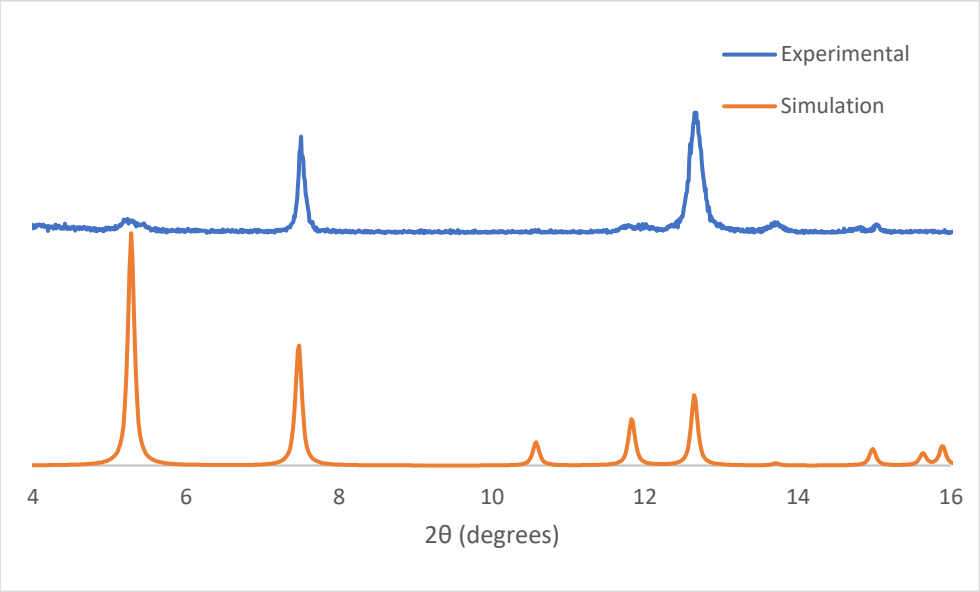
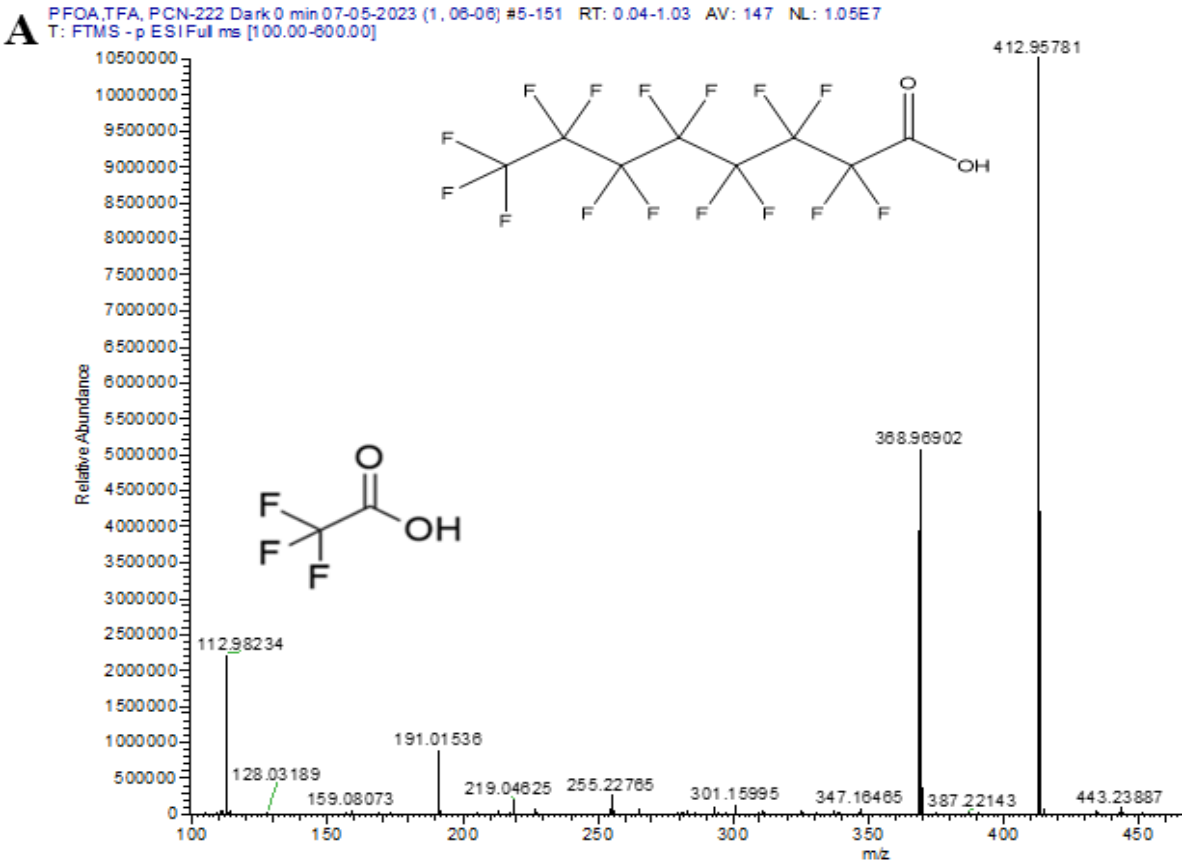
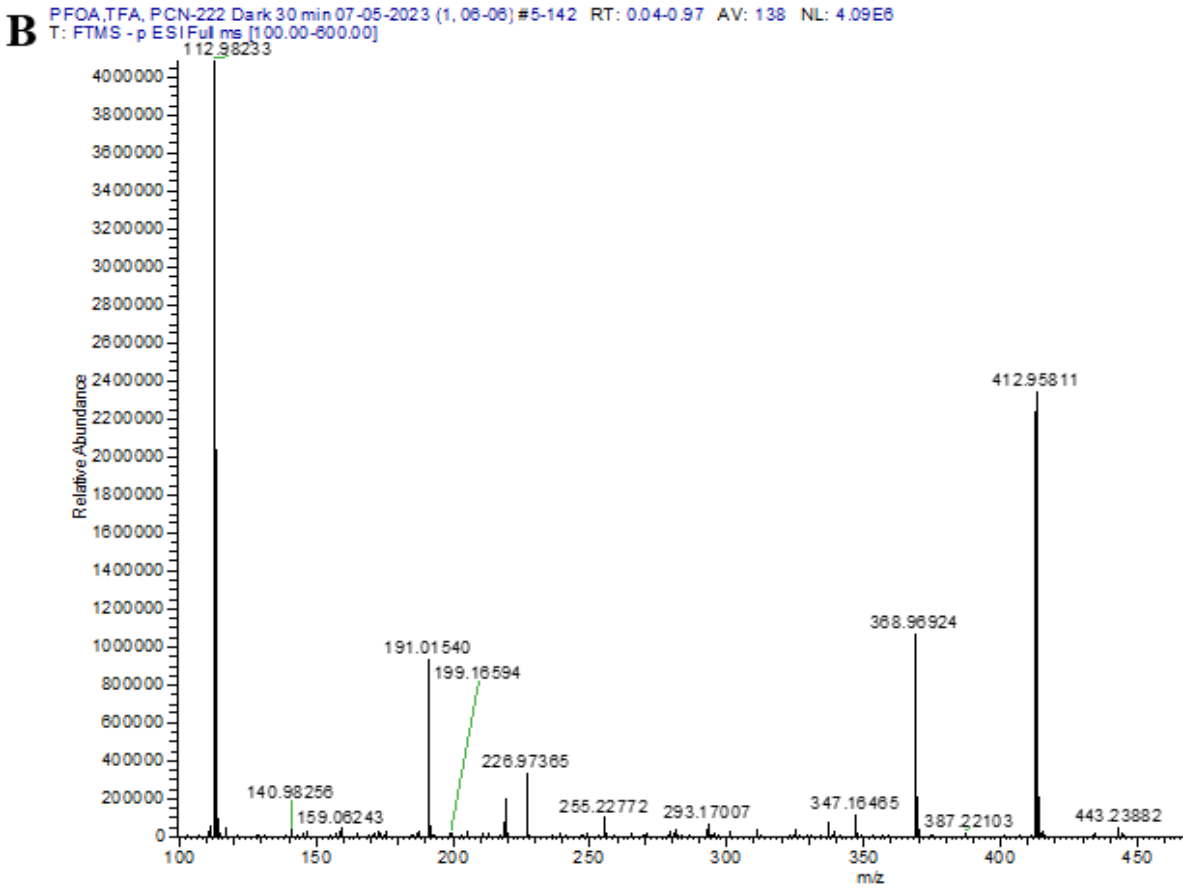


Figure 6. Experimental and simulated PXRD spectra patterns of In-TCPP after storing.

Many zirconium MOFs (Zr-MOFs) have been reported to be stable in diverse applications. Li et al. also reported a zirconium pyrene MOF, NU-1000, which achieved PFOS adsorption without structural decomposition.[3,6] Combining the porphyrin ligand TCPP and Zr nodes, another porphyrin PCN-222 was synthesized with exceptional stability. We first studied PFOA adsorption using PCN-222 in the absence of light. Experiments showed that PCN-222 can decrease PFOA concentration in the solution by 89 $\pm$ 6% after 5 minutes and 97 $\pm$ 2% after 30 minutes (Figure 7). A previous study showed that PFOA was decreased by 80 $\pm$ 27% in the presence of NU-1000 after 30 minutes.[6] Remarkably, PCN-222 is potentially better at adsorption of PFOA than previously reported MOFs.


A
PFOA,TFA, PCN-222 Dark 0 min 07-05-2023 (1, 06-06) #5-151 RT: 0.04-1.03 AV: 147 NL: 1.05E7
T: FTMS - p ESI Full ms [100.00-600.00]
Relative Abundance
m/z
412.95781
368.96902
112.98234
191.01536
128.03189
159.08073
219.04625
255.22765
301.15995
347.16465
387.22143
443.23887


B
PFOA,TFA, PCN-222 Dark 30 min 07-05-2023 (1, 06-06) #5-142 RT: 0.04-0.97 AV: 138 NL: 4.09E6
T: FTMS - p ESI Full ms [100.00-600.00]
Relative Abundance
m/z
112.98233
412.95811
368.96924
191.01540
199.16594
226.97365
140.98256
159.06243
255.22772
293.17007
347.16465
387.22103
443.23882

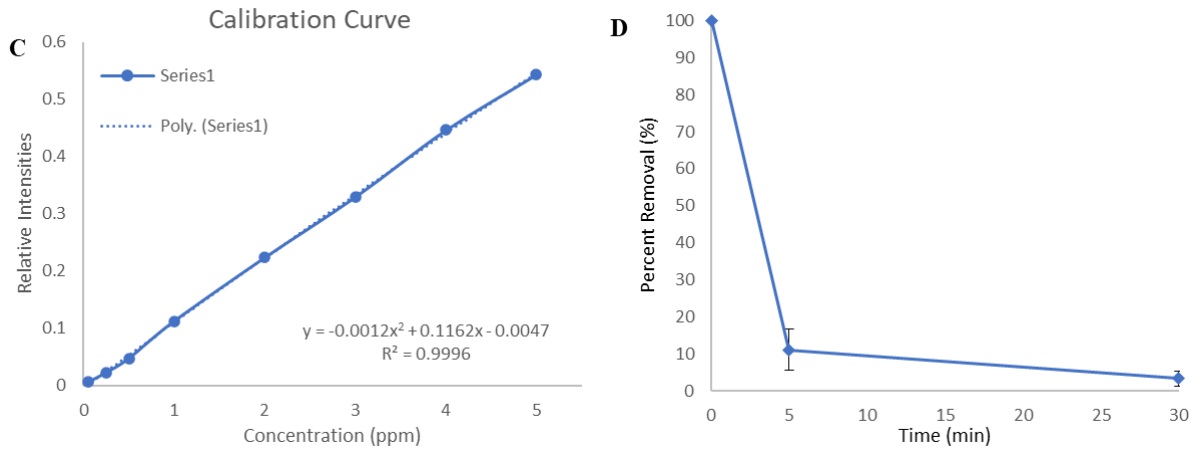
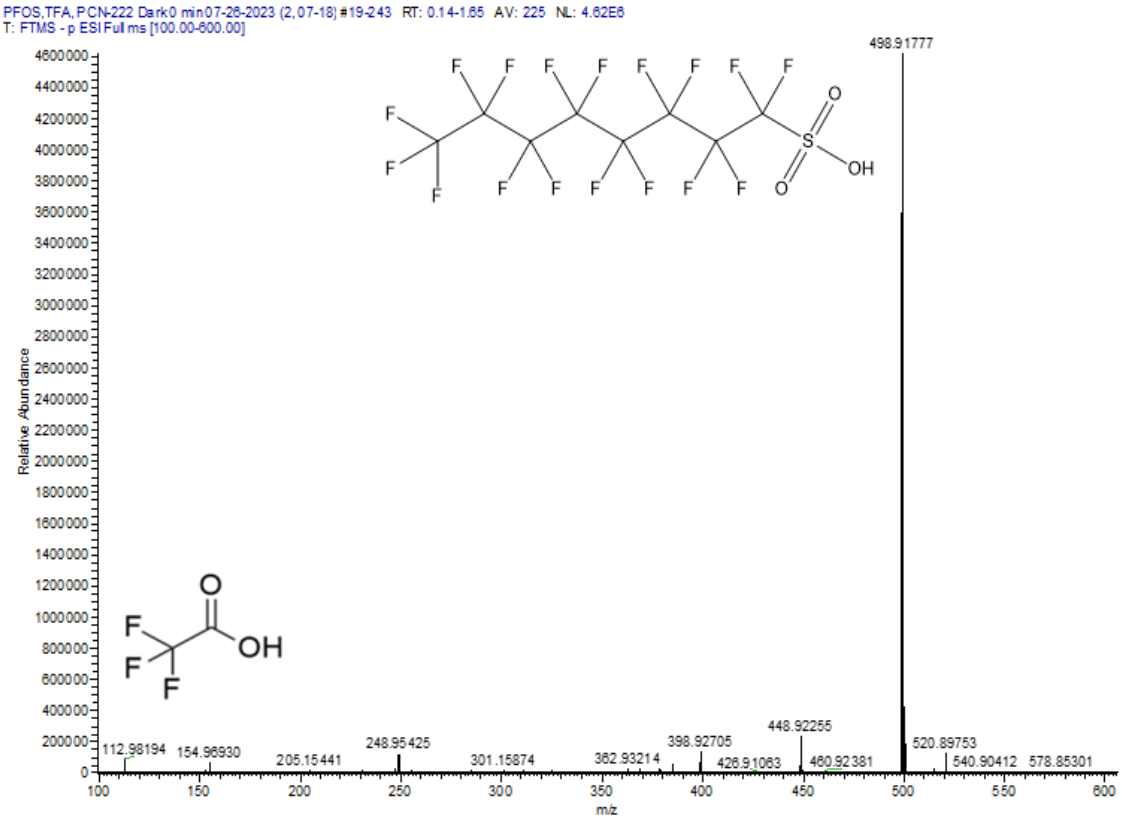


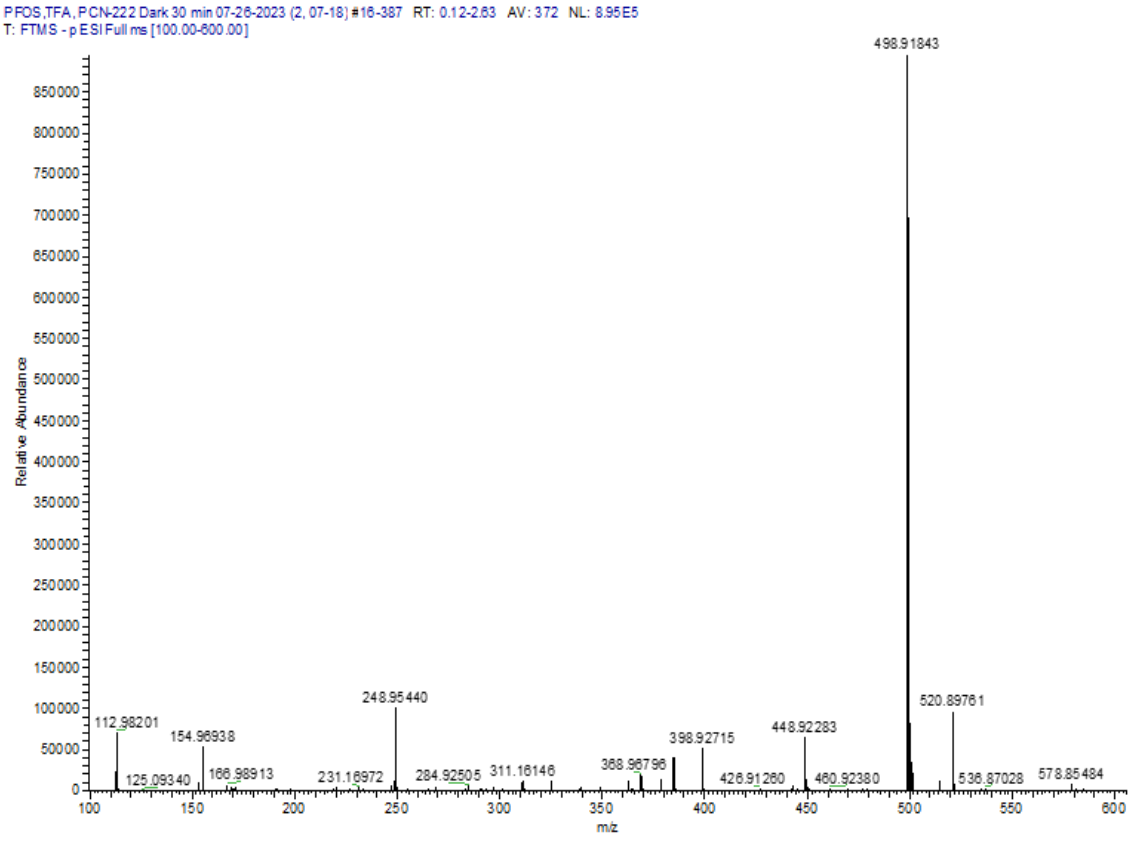
Figure 7. A. LCMS m/z spectra of PFOA at 0 minutes. B. LCMS m/z spectra of PFOA at 30 mintues. C. Calibration Curve of PFOA standards. D. Percent removal of PFOA in solution over time.

Similarly, PCN-222 also effectively removed PFOS from the solution with 87 $\pm$ 5% removal after 5 minutes and 91 $\pm$ 4% removal after 30 minutes (Figure 8). Although PCN-222 did not perform better than previously reported NU-1000 for PFOS removal, PCN-222 is more efficient in removing PFOS compared to previously reported UiO-66 (< 10% removal after 30 minutes) another zirconium MOF.[6] These observations demonstrated that MOFs with different structures, organic ligands and pore sizes may result in different amounts/types of interactions with PFAS and thus exhibited varied removal efficiency for these toxic chemicals.

A


PFOS,TFA, PCN-222 Dark 0 min 07-26-2023 (2, 07-18) #19-243 RT: 0.14-1.65 AV: 225 NL: 4.62E6
T: FTMS - p ESI Full ms [100.00-600.00]
498.91777
448.92255
248.95425
398.92705
520.89753
112.98194
154.96930
205.15441
301.15874
362.93214
426.91063
460.92381
540.90412
578.85301
Relative Abundance
m/z

B


PFOS,TFA, PCN-222 Dark 30 min 07-26-2023 (2, 07-18) #16-387 RT: 0.12-2.63 AV: 372 NL: 8.95E5
T: FTMS - p ESI Full ms [100.00-600.00]
498.91843
248.95440
520.89761
448.92283
398.92715
112.98201
154.96938
125.09340
166.98913
231.16972
284.92505
311.16146
368.96796
426.91260
460.92380
536.87028
578.85484
Relative Abundance
m/z

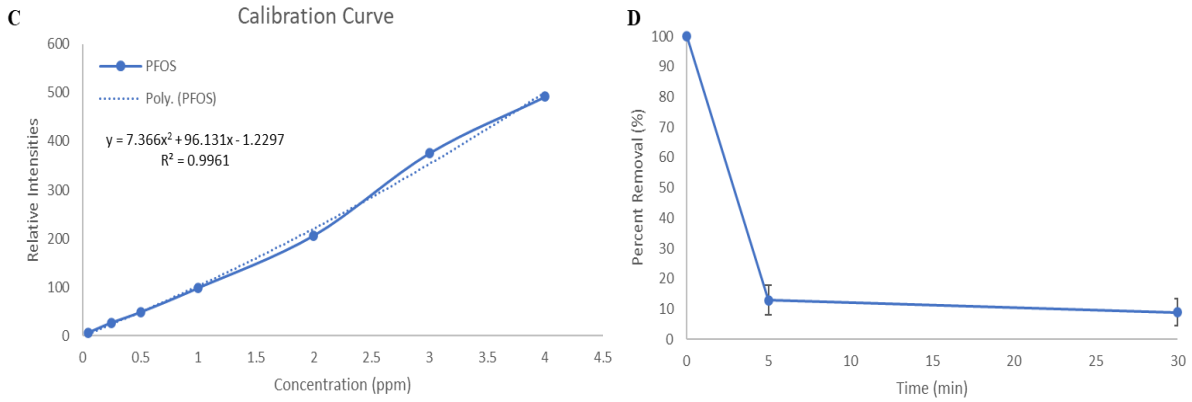
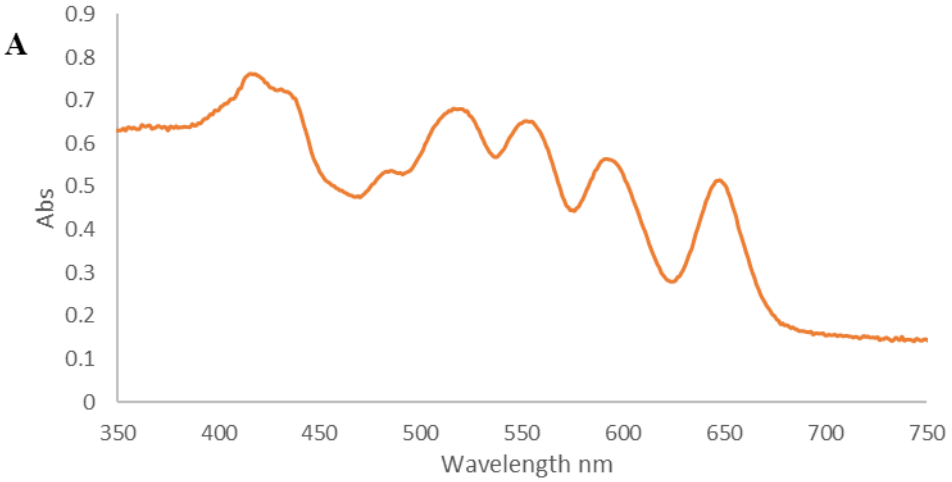
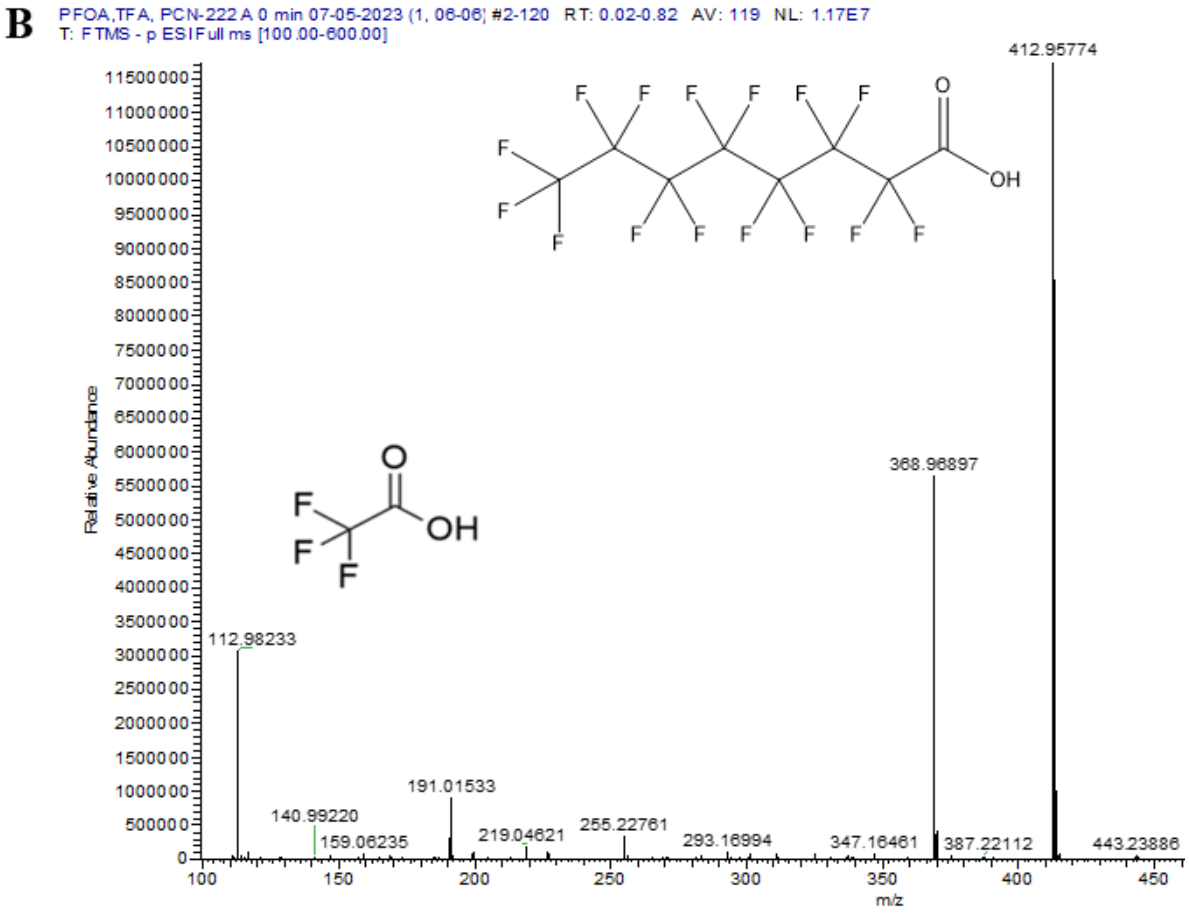


Figure 8. A. LCMS m/z spectra of PFOS at 0 minutes and 30 minutes. B. LCMS m/z spectra of PFOS at 30 minutes. C. Calibration curve of PFOS standards. D. Percent removal of PFOS in solution over time.

Seeing that PCN-222 is capable of adsorbing PFOA and PFOS from water, we next sought to study the potential degradation of these toxic chemicals by the MOF under LED. An integrated sphere UV-Vis was used to determine wavelength of absorbance for PCN-222. Figure 9A shows the UV-Vis spectra with the highest wavelength absorbance at 412 nm, within the blue LED range. Therefore, blue LED was used as a light source for the photocatalysis experiments, where PCN-222 with porphyrin linkers was used as a photocatalyst for ROS generation, which may subsequently decompose PFAS. The experiment setup was similar to that of the adsorption experiment, except that a blue LED was added to photosensitize the MOF in the PFOA/PFOS solution. With blue light irradiation, PCN-222 had decreased PFOA concentration in solution by 89 $\pm$ 4% after 5 minutes and 95 $\pm$ 2% after 30 minutes (Figure 9B-E). The percentage removal at 5 minutes was the same as the experiments ran without light irradiation. However, after 30 minutes, the light-irradiated experiments were 2% lower in removal than without light irradiation. This difference was likely attributed to PFOA decomposition in the presence of ROS generated by the photoactive MOF, PCN-222. However, further experiments are needed to confirm the degradation products.


A
Abs
Wavelength nm
0.9
0.8
0.7
0.6
0.5
0.4
0.3
0.2
0.1
0
350
400
450
500
550
600
650
700
750


B
PFOA,TFA, PCN-222 A 0 min 07-05-2023 (1, 06-06) #2-120 RT: 0.02-0.82 AV: 119 NL: 1.17E7
T: FTMS - p ESI Full ms [100.00-600.00]
Relative Abundance
m/z
412.95774
368.96897
112.98233
191.01533
140.99220
159.06235
219.04621
255.22761
293.16994
347.16461
387.22112
443.23886
OH
O
F

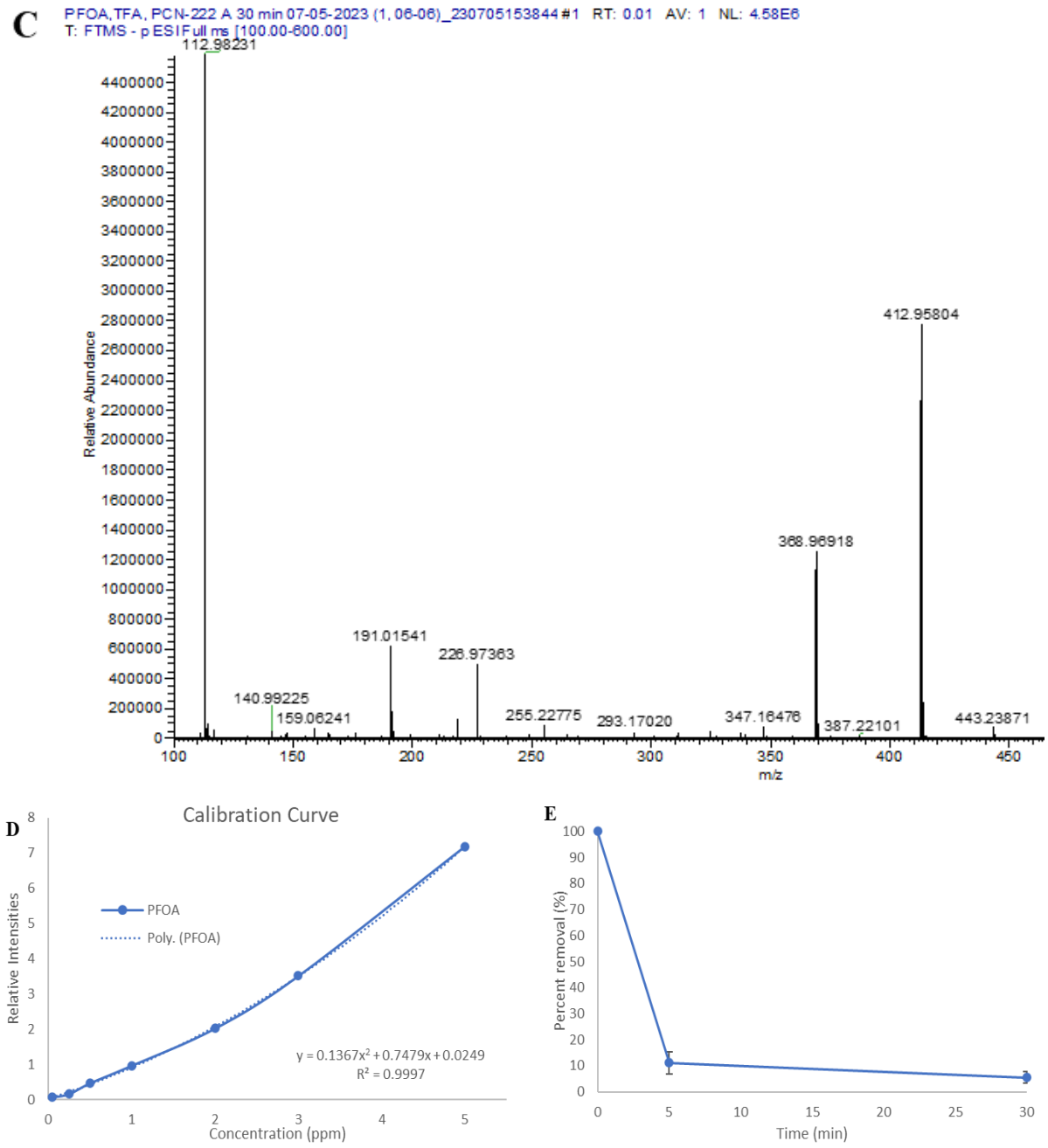
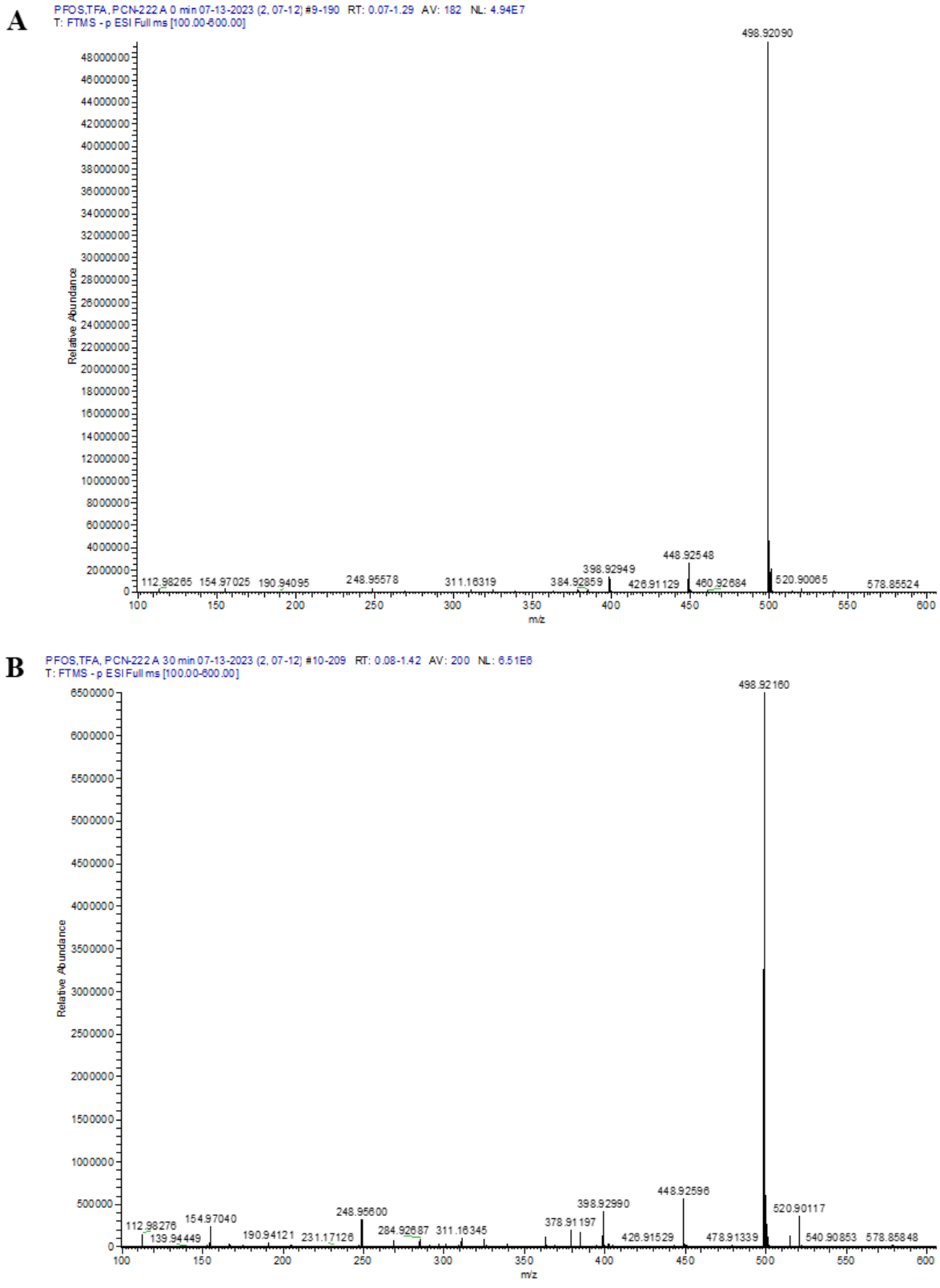


Figure 9. A. The UV-Vis absorption spectrum of PCN-222 suspended in MeOH, measured using an integration sphere accessory. B. LCMS m/z spectra of PFOA at 0 minutes. C. LCMS m/z spectra of PFOA at 30 minutes. D. Calibration curve of PFOA standards. E. Percent removal of PFOA in solution over time.

PCN-222 was also studied with blue LED irradiation for PFOS removal/degradation, resulting in 88 $\pm$ 2% removal after 5 minutes and 91 $\pm$ 1% after 30 minutes (Figure 10). 1% more PFOS was absorbed with blue LED irradiation than without after 5 minutes. However,

after 30 minutes, the removal percentage is the same between the two conditions (with and without LED irradiation).



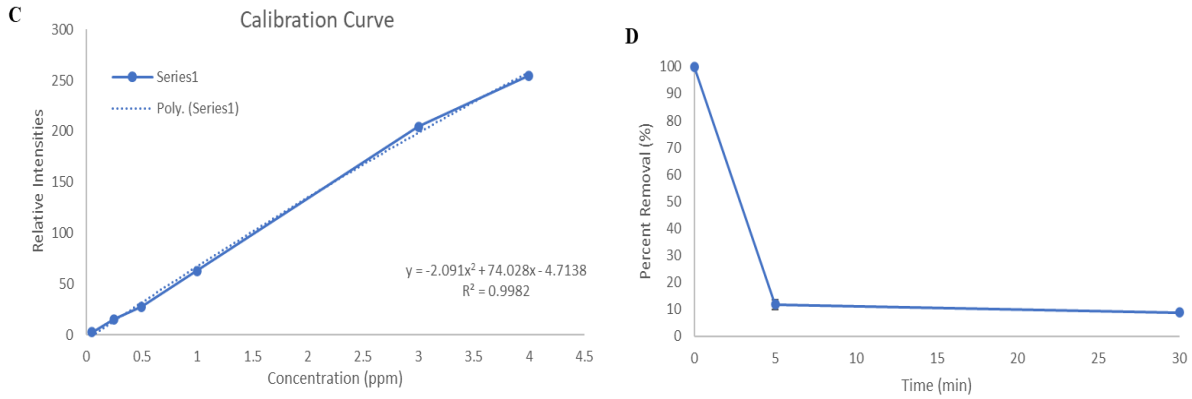


Figure 10. A. LCMS m/z spectra of PFOS at 0 minutes. B. LCMS m/z spectra of PFOS at 30 minutes. D. Calibration curve of PFOS standards. E. Percent removal of PFOS in solution over time.

The regeneration of PCN-222 was also studied by washing the used MOF three times with DI water and another three times with acetone, then characterized by PXRD (Figure 11). The PXRD patterns showed after both PFOA or PFOS adsorption, PCN-222 maintained its structure, indicating its excellent stability. However, the PXRD patterns of PCN-222 after blue LED irradiation for both PFOA and PFOS showed decreased peak intensity or even missed peaks, indicating that the MOF had started to decompose or lose crystallinity. This observation is interesting because PCN-222 was extensively studied for the photocatalytic degradation of various substrates and was reported to be exceptionally stable under various photocatalytic conditions. The decomposition of the MOF may be caused by increased interactions between the PFAS and the MOF under irradiation/elevated temperature.

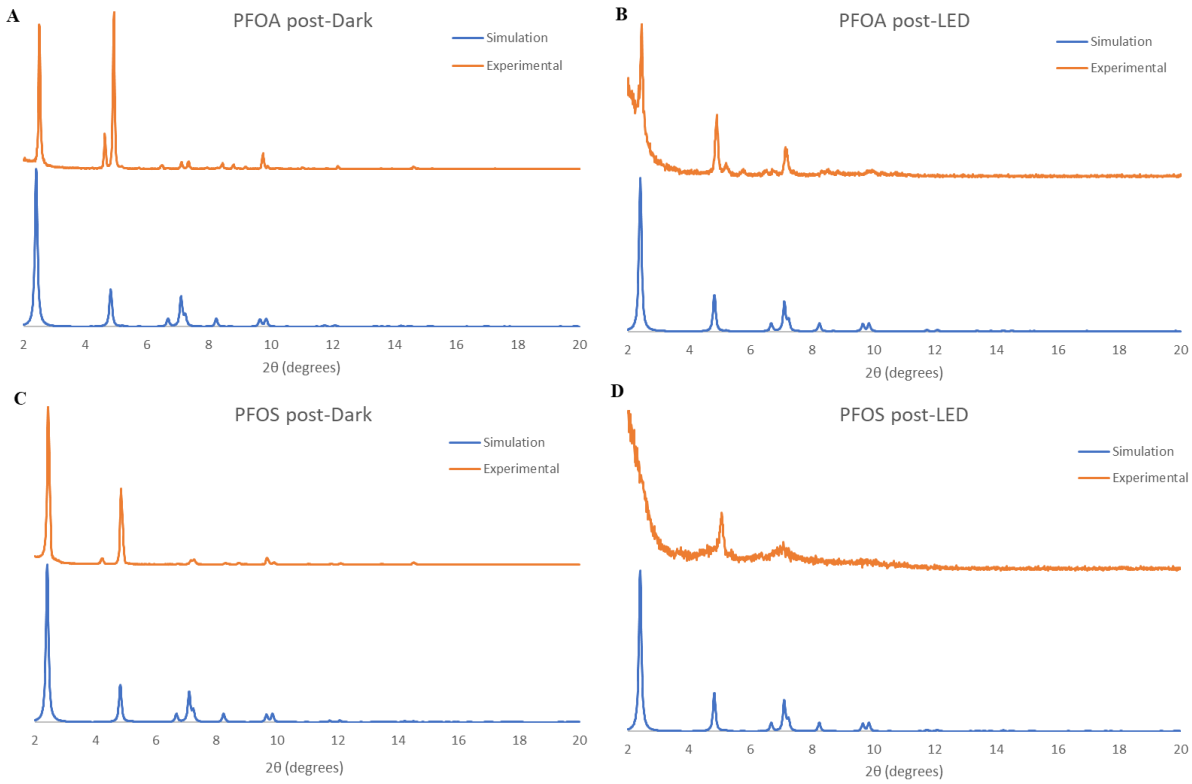


Figure 11. PXRD spectra patterns of PCN-222 after: A. adsorption of PFOA in the dark. B. adsorption of PFOA under blue LED. C. adsorption of PFOS in the dark. D. adsorption of PFOS under blue LED.

CHAPTER 4

Future Work

This study showed that PCN-222 can absorb a considerable amount of PFOA and PFOS from contaminated water solutions. For future work, the maximum quantity of PFOA/PFOS that was stored in the pores of the MOF will be determined through adsorption kinetics. In addition, mechanistic studies will be carried out to understand the mechanisms of adsorption/degradation with and without blue LED irradiation to elucidate a structure-property relationship for MOFs used for PFAS removal. Furthermore, the types of reactive oxygen species generated by MOFs during the photocatalytic process will be determined using trapping experiments. Lastly, the degradation products of PFOA/PFOS will be identified and analyzed using separation columns in the LCMS.

CHAPTER 5

Conclusions

This study demonstrated that PCN-222, a Zr-porphyrin MOF, can effectively remove PFOA and PFOS from contaminated water. The 30 minute removal rate for PFOA and PFOS was 97 $\pm$ 2% and 91 $\pm$ 4%, respectively, comparable or better than the top-performing MOFs reported for this application. For the photocatalysis experiments, PCN-222 removed 95 $\pm$ 2% of PFOA and 91$\pm$ 1% of PFOS after 30 min. Since PCN-222 showed similar performance for the removal of both PFOA and PFOS, this MOF could be used as a promising sorbent for the removal of various groups of PFAS in water treatment. In contrast, the previously reported MOFs, such as NU-1000, are more selective towards PFSA group (PFOS). Further studies on the adsorption of other PFAS and PFAS mixtures by PCN-222 can help better understand the MOF's capability of removing PFAS from contaminated water sources in the environment. Mechanistic studies will elucidate what MOF structure features can affect its selectivity for PFAS adsorption.

REFERENCES

(1) Olatunde, O. C.; Kuvarega, A. T.; Onwudiwe, D. C. Photo enhanced degradation of polyfluoroalkyl and perfluoroalkyl substances. *Heliyon* **2020***, 6*, e05614. DOI: 10.1016/j.heliyon.2020.e05614

(2) Clark, C. A.; Heck, K. N.; Powell, C. D.; Wong, M. S. Highly Defective UiO-66 Materials for the Adsorptive Removal of Perfluorooctanesulfonate. *ACS Sustain. Chem. Eng.* **2019***, 7*, 6619.

(3) Li, X.; Zhang, P.; Jin, L.; Shao, T.; Li, Z.; Cao, J. Efficient Photocatalytic Decomposition of Perfluorooctanoic Acid by Indium Oxide and Its Mechanism. *Environ. Sci. Technol.* **2012***, 46*, 5528-5534.

(4) Liu, X.; Xu, B.; Duan, X.; Hao, Q.; Wei, W.; Wang, S.; Ni, B. Facile preparation of hydrophilic In2O3 nanospheres and rods with improved performances for photocatalytic degradation of PFOA. *Environ. Sci. Nano* **2021***, 8*, 1010.

(5) Russo, V.; Hmoudah, M.; Broccoli, F.; Iesce, M. R.; Jung, O.; Serio, M. D. Applications of Metal Organic Frameworks in Wastewater Treatment: A Review on Adsorption and Photodegradation. *Front. Chem. Eng.* **2020***, 2*. DOI: 10.3389/fceng.2020.581487.

(6) Li, R.; Alomari, S.; Stanton, R.; Wasson, M. C.; Islamoglu, T.; Farha, O. K.; Holsen, T. M.; Thagard, S. M.; Trivedi, D. J.; Wriedt, M. Efficient Removal of Per- and Polyfluoroalkyl Substances from Water with Zirconium-Based Metal–Organic Frameworks. *Chem. Mater.* **2021***, 33*, 3276.

(7) Merino, N.; Qu, Y.; Deeb, R. A.; Hawley, E. L.; Hoffmann, M. R.; Mahendra, S. Degradation and Removal Methods for Perfluoroalkyl and Polyfluoroalkyl Substances in Water. *Environ. Eng. Sci.* **2016***, 33*, 615-649.

(8) Feng, D.; Gu, Z.; Li, J.; Jiang, H.; Wei, Z.; Zhou, H. Zirconium-Metalloporphyrin PCN-

222: Mesoporous Metal-Organic Frameworks with Ultrahigh Stability as Biomimetic Catalysts. *Angew. Chem. Int. ed.* **2012***, 51*, 10307-10310.

(9) Keum, Y.; Park, S.; Chen, Y.; Park, J. Titanium-Carboxylate Metal-Organic Framework Based on an Unprecedented Ti-Oxo Chain Cluster. *Angew. Chem. Int. ed.* **2018***, 57*, 14852-14856.

(10) Rhauderwiek, T.; Waitschat, S.; Wuttke, S.; Reinsch, H.; Bein, T.; Stock, N. Nanoscale Synthesis of Two Porphyrin-Based MOFs with Gallium and Indium. *Inorg. Chem.* **2016***, 55*, 5312-5319.

(11) Hao, Y.; Papazyan, E.; Ba, Y.; Liu, Y. Mechanism-Guided Design of Metal-Organic Framework Composites for Selective Photooxidation of a Mustard Gas Simulant under Solvent-Free Conditions. *ACS Catal.* **2022**, *12*, 363−371.